Available online at www.sciencedirect.com

SCIENCE DIRECT®

Tectonophysics 403 (2005) 95–115

TECTONOPHYSICS

www.elsevier.com/locate/tecto

Empirical relationships between aftershock area dimensions and magnitude for earthquakes in the Mediterranean Sea region

Konstantinos I. Konstantinou[a,b,*], Gerassimos A. Papadopoulos[b], Anna Fokaefs[b], Katerina Orphanogiannaki[b]

[a]*Institute of Earth Sciences, Academia Sinica, P.O. Box 1-55, Nankang Taipei, Taiwan*
[b]*Institute of Geodynamics, National Observatory of Athens, P.O. Box 20048, 118 10, Athens, Greece*

Received 9 November 2004; received in revised form 23 March 2005; accepted 5 April 2005
Available online 2 June 2005

Abstract

Fault dimension estimates derived from the aftershock area extent of 36 shallow depth (≤31 km) earthquakes that occurred in the Mediterranean Sea region have been used in order to establish empirical relationships between length, width, area and surface-wave/moment magnitude. This dataset consists of events whose aftershock sequence was recorded by a dense local or regional network and the reported location errors did not exceed on average 3–5 km. Surface-wave magnitudes for these events were obtained from the NEIC database and/or published reports, while moment magnitudes as well as focal mechanisms were available from the Harvard/USGS catalogues. Contrary to the results of some previously published studies we found no evidence in our dataset that faulting type may have an effect on the fault dimension estimates and therefore we derived relationships for the whole of the dataset. Comparisons, by means of statistical *F*-tests, of our relationships with other previously published regional and global relationships were performed in order to check possible similarities or differences. Most such comparisons showed relatively low significance levels (<95%), since the differences in source dimension estimates were large mainly for magnitudes lower than 6.5, becoming smaller with increasing magnitude. Some degree of similarity, however, could be observed between our fault length relationship and the one derived from aftershock area lengths of events in Greece, while a difference was found between our regional and global fault length relationships. A calculation of the ratio defined as the fault length, derived from our relationships, to the length estimated from regional empirical relationships involving surface ruptures showed that it can take a maximum value of about 7 for small magnitudes while it approaches unity at Ms ~7.2. When calculating the same ratio using instead global empirical relationships we see the maximum value not exceeding 1.8, while unity is reached at Mw ~7.8, indicating the existence of a strong regional variation in the fault lengths of earthquakes occurring in the Mediterranean Sea region. Also, a relationship between the logarithms of the rupture area and seismic moment is established and it is inferred that there is some variation of stress drop as a function of seismic moment. In particular, it is observed that for magnitudes

* Corresponding author. Institute of Earth Sciences, Academia Sinica, P.O. Box 1-55, Nankang Taipei, Taiwan.
E-mail address: kostas@earth.sinica.edu.tw (K.I. Konstantinou).

0040-1951/$ - see front matter © 2005 Elsevier B.V. All rights reserved.
doi:10.1016/j.tecto.2005.04.001

lower than 6.6 the stress drop fluctuates around 10 bar, while for larger magnitudes the stress drop reaches a value as high as 60 bar.
© 2005 Elsevier B.V. All rights reserved.

Keywords: Aftershock area; Fault dimensions; Surface ruptures; Mediterranean; Stress drop; Seismic hazard

1. Introduction

Observations of surface ruptures usually accompany most large earthquakes ($M>6.5$) and the logarithms of their corresponding dimensions (primarily length) have been found to relate linearly to earthquake magnitude (e.g. Tocher, 1954; Otsuka, 1964). This empirical relationship between source dimensions and magnitude was later justified theoretically by Kanamori and Anderson (1975) in terms of crack and dynamic dislocation models. As more surface rupture observations were accumulating and local or surface-wave magnitudes could be determined routinely for each earthquake, it was possible to model these data using standard least-squares regression methods (Mark, 1977; Bolt, 1978). Thus, the empirical relationships that were established could predict not only the fault dimensions for a given magnitude, but also the maximum magnitude based on known fault dimensions. These relationships proved extremely useful to geotechnical, seismic hazard assessment and seismotectonic applications.

The use of surface ruptures as primary data for fault dimension estimation exhibit, however, two important problems. First, field observations of ground breakage may not always express the manifestation of the seismogenic fault reaching the surface of the Earth, but rather secondary ground deformation phenomena (like superficial cracks, liquefaction, landslides, etc.). Second, surface rupture lengths usually fail to estimate the actual length of the seismogenic fault by a factor that is inversely proportional to the magnitude of the earthquake (Wells and Coppersmith, 1994). The former problem has also the effect of restricting the magnitude range of the data, since only large events with well-defined surface rupture zones could be used in the least-squares regressions. On the other hand, extrapolating such regressions for magnitudes smaller than the lower values of the data that were used to derive them, has been found to produce incorrect fault dimension estimates (Darragh and Bolt, 1987).

The advances in the field of seismic instrumentation and the installation of regional and local seismic networks in many parts of the world made possible the recording of large, but also moderate to small earthquakes ($M\leq6$) including their aftershock sequences. This development permitted the estimation of fault dimensions, i.e. length and downdip width, from the extent of the aftershock zone and their use in the determination of more accurate regression lines that extend also to smaller magnitude intervals (e.g. Liebermann and Pomeroy, 1970). The introduction and widespread use of the moment magnitude scale (Hanks and Kanamori, 1979) rather than the surface-wave magnitude also helped to overcome problems concerning the saturation of the scale above a certain threshold, as well as the fluctuation of the magnitude value due to azimuthal distribution and epicentral distance when using data from different stations.

A comparison of these empirical relationships from many different regions around the world has showed that earthquakes with similar magnitudes seem to correspond to faults with significantly different dimensions (Acharya, 1979; Dowrick and Rhoades, 2004). Authors have suggested many reasons for this regional variation, including differences in seismic efficiency from one area to another (Acharya, 1979) or variations of the rigidity modulus value (Bonilla et al., 1984). However, a geologically plausible explanation based on the physical properties of the different fault zones around the world is yet to be proposed. Hereafter we will refer to empirical relationships derived from worldwide datasets as ‘global’, while those obtained from datasets from a specific region as ‘regional’.

This article describes the application of a statistical regression analysis to a sample of 36 earthquakes that occurred in the Mediterranean Sea region, in an effort to obtain empirical relationships of aftershock area

dimensions (length, width, area) as a function of both surface-wave (Ms) and moment magnitude (Mw). The resulting regression lines are then compared through the use of a statistical *F*-test, not only to previously published relationships for areas around the Mediterranean, but also to global relationships. Also, a comparison is made between our regression results and those obtained using surface ruptures rather than aftershock area length (also referred to in this study as subsurface rupture length). Finally, we make an inference about the amount of stress drop in our dataset after establishing an empirical relationship between the logarithms of rupture area and seismic moment and compare our results with those reported in an earlier study by Kiratzi et al. (1985).

2. Data selection and characteristics

Studies of aftershock sequences of 36 events that occurred in regions around the Mediterranean Sea in the period 1954–2001 have been used in order to determine rupture length, width and area from the extent of their aftershock zone. The majority of these events had a hypocentral depth equal to or less than 15 km, while the depth of the deepest event did not exceed 31 km (Fig. 1). Following Wells and Coppersmith (1994) we estimate the subsurface rupture length as the length of the best-defined aftershock zone, ignoring any activity that is away from the main cluster(s) of epicentres by more than the reported horizontal location error in each case. Similarly, we estimate the width by measuring the surface extent of the epicentres in a perpendicular direction to that of the subsurface rupture length. We chose this way of width estimation instead of the downdip width for two reasons: first, vertical errors were almost always greater than the corresponding horizontal ones, making in many cases such a determination uncertain; second, in cases where the downdip width could be reliably identified it was either the same with our initial width estimate, or the difference was of the same order with the vertical location error. We consider the rupture area as simply the product of subsurface rupture length and width for each event. Tables 1 and 2 give a summary of the source parameters and corresponding references for the events used in this study. Appendix A includes a more detailed description of the available information used in length/width estimations for each event separately.

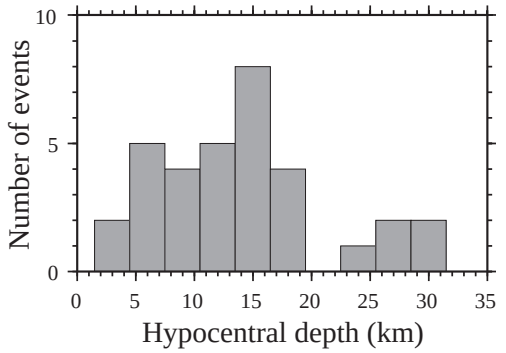

Fig. 1. Distribution of hypocentral depths for the events considered in this study. Depth values have been obtained from the global teleseismic relocation database of Engdahl et al. (1998) and its subsequent updates (see also Table 1).

Most of the events in our dataset comply to the following criteria: (1) the recording of the aftershock sequence by a dense regional or local network with a good azimuthal coverage; for 24 events (67%) of our dataset the aftershock location was perfomed using data from local networks while only for 12 events (33%) this was done using regional network data, (2) reported epicentral location errors that did not exceed on average 3–5 km (with the only exception of event 2—see Appendix A). It should be noted that none of the events we selected is associated with subduction processes.

Another factor that has been taken into account when selecting the data, was the total duration of recording of the aftershock sequence, since only aftershocks occurring during the first few days after the mainshock define the true co-seismic rupture area (Kanamori and Anderson, 1975). Even though many of the aftershock sequences we have selected also conform to this factor, some of them extended to a period of more than 10 days. We chose to include these events to our analysis as well, since at least one of the following conditions was found to be true: (1) dimension estimates derived for different time periods during the aftershock sequence indicated that aftershock area expansion is not significant, (2) the estimated dimension values are similar with those derived a few days after the mainshock for another event of our dataset having the same magnitude.

Table 1
List of events that were used in this study and their corresponding source parameters

	Date	FT	H (km)	Ms	Mw	L (km)	W (km)	A (km^2)
1	1954/09/09	T	–	6.5	–	30	10	300
2	1968/02/19	S	9	7.2	7.0	95	–	–
3	1976/05/06	T	–	6.5	6.5	25	15	375
4	1978/06/20	N	8	6.4	6.3	28	14	392
5	1979/04/15	S	15	6.9	7.0	83	23	1909
6	1980/02/29	O	–	–	5.2	6	3	18
7	1980/07/09	N	17	6.3	6.6	40	13	520
8	1980/10/10	T	12	7.2	7.1	90	25	2250
9	1980/11/23	N	6	6.8	6.9	50	14	700
10	1981/02/24	N	16	6.6	6.6	32	15	480
11	1981/12/19	S	14	7.2	6.9	90	30	2700
12	1982/01/18	S	15	6.9	6.6	60	30	1800
13	1983/01/17	S	6	7.0	6.9	55	30	1650
14	1983/08/06	S	15	6.9	6.7	51	25	1275
15	1984/04/29	N	7	5.2	5.7	18	7	126
16	1985/10/27	S	30	5.9	5.8	25	11	275
17	1986/09/13	N	16	5.8	6.0	15	10	150
18	1988/10/16	S	17	5.8	5.9	17	9	153
19	1988/12/07	T	7	6.7	6.8	46	12	552
20	1990/05/05	S	2	5.6	5.8	20	8	160
21	1992/03/13	S	26	6.8	6.7	30	8	240
22	1992/10/12	N	23	5.4	5.8	25	12	300
23	1992/11/18	N	11	5.7	5.9	25	15	375
24	1993/07/14	O	19	5.4	5.6	14	7	98
25	1994/05/26	S	4	5.9	6.0	30	10	300
26	1995/05/13	N	13	6.6	6.6	35	14	490
27	1995/06/15	N	27	6.4	6.5	27	11	297
28	1995/10/01	N	31	6.1	6.4	35	20	700
29	1995/11/22	S	13	7.1	7.2	70	23	1610
30	1996/04/03	N	14	4.7	5.1	9	3	27
31	1997/09/26	N	7	6.0	6.0	25	11	275
32	1998/06/27	S	16	6.2	6.3	32	8	256
33	1999/08/17	S	17	7.8	7.6	155	20	3100
34	1999/09/07	N	9	5.8	6.0	25	14	350
35	1999/11/12	S	10	7.5	7.2	65	22	1430
36	2001/07/26	S	19	6.5	6.4	27	14	378

Column FT represents the faulting type (S: Strike-slip, N: Normal, T: Thrust, O: Oblique-slip), while column H represents hypocentral depth estimates taken from Engdahl et al. (1998) (events 1, 3, 6 did not have a well-constrained depth).

For almost all the events in our dataset both the surface-wave magnitude (Ms) and the moment magnitude (Mw) are known with the exception of events 1 and 6, where only the Ms or Mw were available in each case. Event magnitudes have been compiled using as the primary source the published aftershock studies and these values were then compared to the ones given by NEIC for Ms and the Harvard/USGS

Table 2
Areas of occurrence and references of source parameters for the events listed in Table 1

	Region	References
1	Algeria	Dewey (1990)
2	N. Aegean Sea	Drakopoulos and Economides (1972); Taymaz et al. (1991)*
3	Friuli, Italy	Cipar (1980); Aoudia et al. (2000)
4	N. Greece	Soufleris et al. (1982); Carver and Bollinger (1981); Kulhanek and Meyer (1981)
5	Montenegro	Console and Favali (1981); Karakaisis et al. (1984)
6	S. France	Gagnepain-Beyneix et al. (1982)
7	Volos, Greece	Papazachos et al. (1983)
8	Algeria	Meghraoui et al. (1988); Dewey (1990)
9	Irpinia, Italy	Scarpa and Slejko (1982); Deschamps and King (1983); Amato and Selvaggi (1993); Giardini (1993)*
10	C. Greece	Papazachos et al. (1984a); Kim et al. (1984)*; King et al. (1985)
11	C. Aegean Sea	Papazachos et al. (1984b); Kiratzi et al. (1991)*
12	N. Aegean Sea	Papazachos et al. (1984b)
13	W. Greece	Scordilis et al. (1985); Baker et al. (1997)*
14	N. Aegean Sea	Rocca et al. (1985); Kiratzi et al. (1991)*
15	Perugia, Italy	Haessler et al. (1988)
16	Algeria	Bounif and Dorbath (1998)
17	C. Greece	Papazachos et al. (1988); Lyon-Caen et al. (1988)
18	W. Greece	Karakostas et al. (1993)
19	Armenia	Dorbath et al. (1992); Balassanian et al. (1995)
20	Potenza, Italy	Azzara et al. (1993); Ekström (1994)*
21	N. Turkey	Fuenzalinda et al. (1997); Eyidogan and Akinci (1999)
22	Cairo, Egypt	Elenean et al. (2000)
23	W. Greece	Hatzfeld et al. (1996)
24	Patra, Greece	Karakostas et al. (1994)
25	N. Morocco	Calvert et al. (1997); El-Alami et al. (1998)
26	Kozani, Greece	Hatzfeld et al. (1997)
27	Aegio, Greece	Tselentis et al. (1996); Bernard et al. (1997)
28	Dinar, Turkey	Oncel et al. (1998); Pinar (1998)
29	Aqaba, Syria	Fattah et al. (1997); Klinger et al. (1999); Hofstetter et al. (2003)
30	Irpinia, Italy	Cocco et al. (1999)
31	Umbria, Italy	Amato et al. (1998); Ekström et al. (1998)*; Deschamps et al. (2000); Cattaneo et al. (2000)
32	Adana, Turkey	Aktar et al. (2000)
33	Izmit, Turkey	Güllen et al. (2002); Polat et al. (2002); Ozalaybay et al. (2002); Ito et al. (2002)
34	Athens, Greece	Tselentis and Zahradnik (2000); Papadopoulos et al. (2001); Papadimitriou et al. (2002)
35	Düzce, Turkey	Bayrak and Öztürk (2004)
36	C. Aegean Sea	Papadopoulos et al. (2002); Roumelioti et al. (2003)

References highlighted with an asterisk indicate focal mechanism/moment tensor studies.

catalogues for Mw. In only one case (event 2) the moment magnitude was calculated from the scalar moment M_0 value obtained after waveform inversion of teleseismic data by Taymaz et al. (1991), using the equation of Hanks and Kanamori (1979)

$$\mathrm{Mw} = 2/3 \log M_0 - 10.7 \quad (1)$$

As it was expected the differences between the published and catalogue-based values of moment magnitude for all the events in our dataset never exceeded 0.1 units. This was also true for most of the surface-wave magnitudes, even though there were two cases where significant differences were found and we briefly summarise them below:

- For event 8, Dewey (1990) gives a range of estimated Ms values from different stations between 7.3 and 7.7, but adopts Ms=7.3. The same value is adopted by Meghraoui et al. (1988) while NEIC reports Ms=7.2 for this event. In our regression we preferred to use the NEIC magnitude value that is also not significantly different from the one the authors finally adopted.
- For event 13, Scordilis et al. (1985) give an Ms range of 6.6–7.2 while NEIC gives Ms=7.0. In our regression we chose to use a mean value of 6.9 which is also close to the NEIC estimate.

In order to check for a possible saturation of the surface-wave magnitude scale, we plotted the Mw against Ms for the 34 events that both magnitude values were available (Fig. 2). The resulting diagram shows no signs of a saturation and also indicates that the two magnitude estimates are to a good approximation equal. This is consistent with previous studies that report that surface-wave magnitude saturation is not significant for Ms<8 (Kanamori, 1977; Howell, 1981) and also the results of Kanamori (1983) that suggest that Ms and Mw are approximately equal for the range 5.0≤Ms≤7.5. We find that the standard deviation of the difference between each pair of Ms and Mw values in our data is 0.20, only slightly higher than the one that Wells and Coppersmith (1994) calculated for their global dataset (~0.19). The equation that relates the two magnitude scales for our data was found to be after the regression,

$$\mathrm{Mw} = 0.76(\pm 0.03)\mathrm{Ms} + 1.53(\pm 0.19), \quad r = 0.97. \quad (2)$$

This relationship gives similar values of Mw with the relationship suggested by Papazachos et al. (1997) for earthquakes in the Aegean Sea region, which is

$$\mathrm{Mw} = 0.56\mathrm{Ms} + 2.66, \qquad 4.2 \le \mathrm{Ms} \le 6.0 \quad (3)$$

with the standard deviation of the difference between the two estimates being 0.1.

Focal mechanisms are available for all of the earthquakes in our dataset and they are either derived from a particular study (for events occurring before 1977), or obtained from the Harvard/USGS catalogues for events after 1977 (see also Table 1). In cases where both kinds of focal mechanisms were available, a comparison was made in order to check the consistency of the individual solutions. The faulting type for the events of our dataset was normal faulting for 14 events (39%), thrust faulting for 4 events (11%), strike-slip faulting for 16 events (44%) and oblique-slip faulting for only 2 events (6%).

There seems to be no agreement among authors as to whether the faulting type of an earthquake has a significant effect on its source dimensions or not. Even though Wells and Coppersmith (1994) produced different empirical relationships as a function of faulting type, they concluded that these were not statistically different at a 95% confidence level. In a more recent study Dowrick and Rhoades (2004) reached to the same conclusion for their New Zealand regional dataset as well. On the contrary, Bonilla et al. (1984) and Vakov (1996) observed a significant

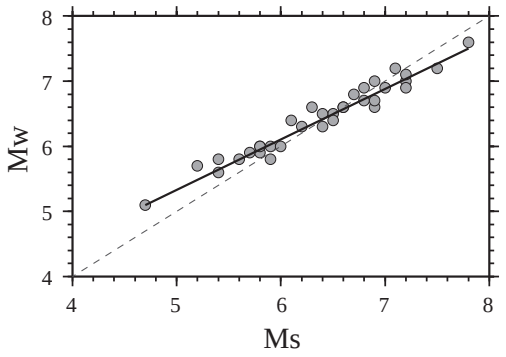

Fig. 2. Moment magnitude (Mw) versus surface-wave magnitude (Ms) for the 34 events in our dataset that both values are available. Dashed line indicates the diagonal, where the two values are equal, while the solid line indicates the least-squares fit to the data.

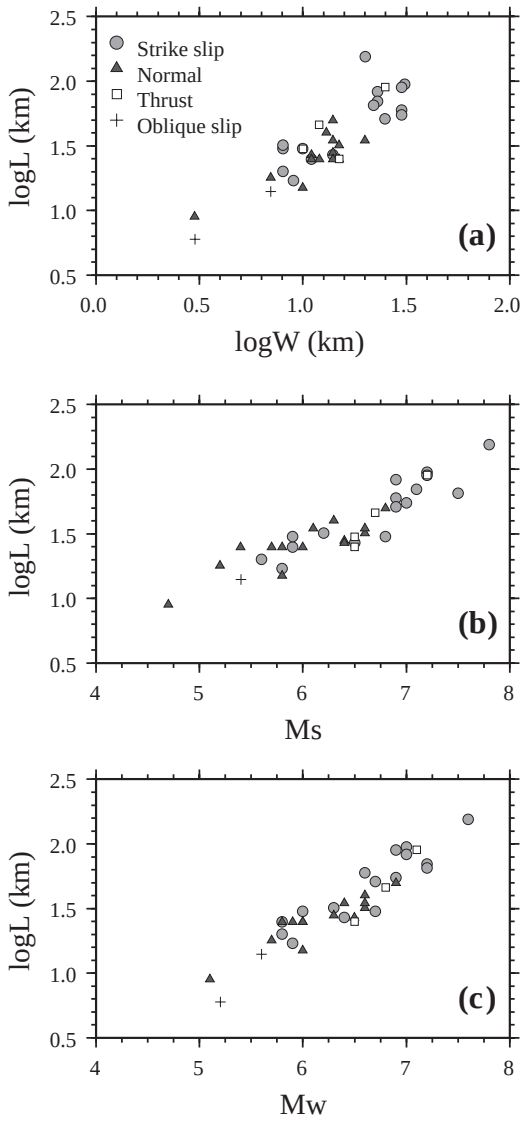

Fig. 3. Diagrams of our dataset based on faulting type for: (a) the logarithm of fault length versus logarithm of fault width, (b) the logarithm of fault length versus surface magnitude, (c) the logarithm of fault length versus moment magnitude.

difference in the relationships they derived for different faulting types using global data. We investigated the possibility that the source dimensions of our data may depend on slip motion by plotting log L against log W and also by plotting log L–Ms/Mw for all events belonging to the three different faulting groups (Fig. 3). An inspection of the diagrams shows no significant differentiation of source dimensions due to slip motion and therefore we did not opt for separate regressions based on the faulting type of the data.

3. Regression analysis

The general relationship that we have used in all regressions that involved fault dimensions and magnitude, is the one that connects the logarithm of length, width, area with Ms or Mw:

$$\log(L, W, A) = a + b(\mathrm{Ms}, \mathrm{Mw}) \quad (4)$$

We evaluated the regression coefficients a and b using two different approaches: (1) the straightforward application of the maximum likelihood least-squares method to our dataset (Press et al., 1992), (2) the production of 5000 'pseudosynthetic' datasets generated using the bootstrap method (Efron and Tibshirani, 1993) where for each one of them the regression coefficients were calculated and their average value was taken as the final estimate of a and b (while the standard deviation serves as an estimate of the uncertainty).

Both approaches gave the same estimates for the values of the regression coefficients and for their corresponding uncertainties (Table 3). Fig. 4 shows the diagrams of the logarithm of length/width/area versus Ms/Mw and the resulting best-fitting lines. These results indicate that the length/area versus magnitude data appear to have the highest correlation

Table 3
Summary of the values obtained in this study for the regression lines coefficients a and b, linear correlation coefficients r and the corresponding uncertainties $\delta(a, b)$ for Subsurface Rupture Length (SbRL), Subsurface Rupture Width (SbRW) and Rupture Area (RA). All linear correlation coefficients were found to be significant at a 99% confidence level

Relationship	a	δa	b	δb	r
SbRL					
log $L = a + b$Ms	−0.69	0.18	0.35	0.02	0.90
log $L = a + b$Mw	−1.49	0.21	0.47	0.03	0.92
SbRW					
log W $= a + b$Ms	−0.48	0.21	0.25	0.03	0.79
log $W = a + b$Mw	−1.07	0.27	0.34	0.04	0.80
RA					
log $A = a + b$Ms	−1.17	0.34	0.60	0.05	0.89
log $A = a + b$Mw	−2.57	0.43	0.81	0.06	0.90

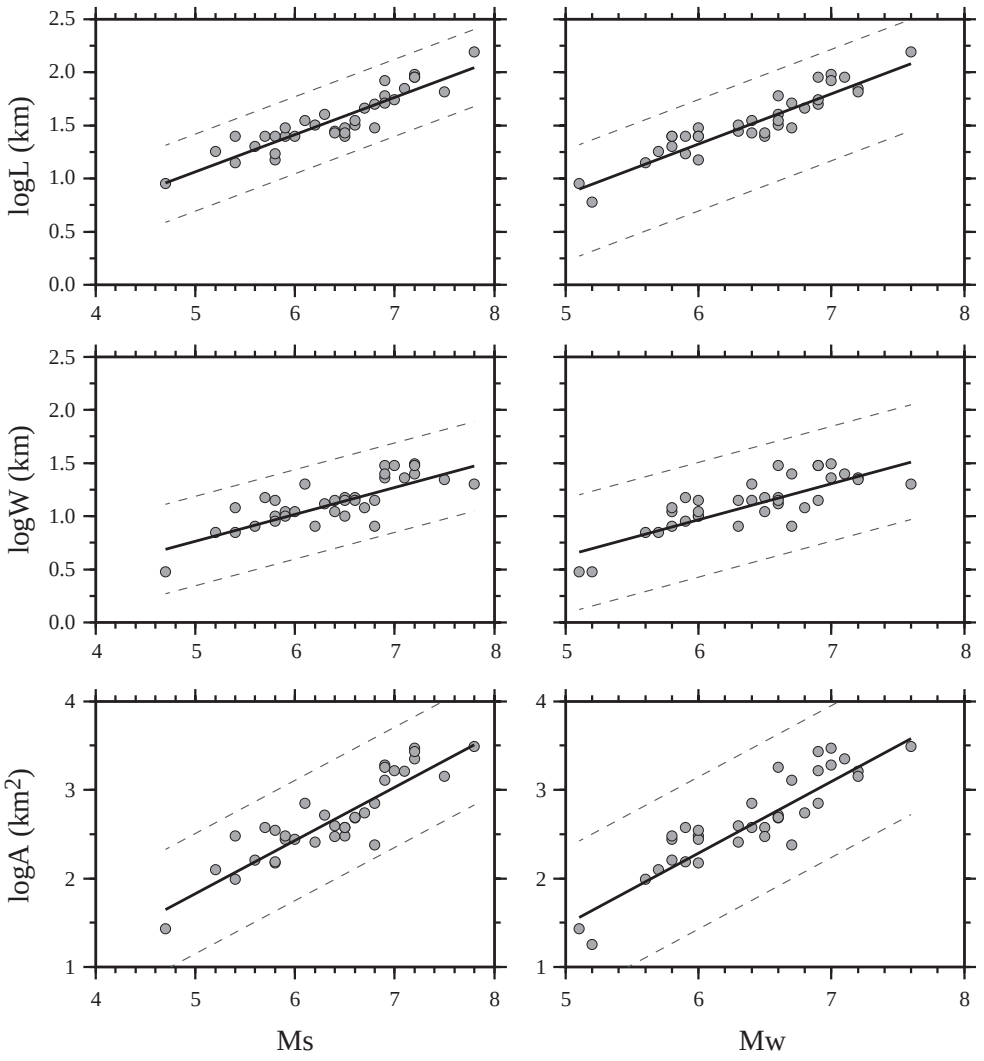

Fig. 4. Diagrams of the logarithm of subsurface rupture length/width/area versus surface-wave and moment magnitude. Solid lines indicate the least-squares fit to the data, while dashed lines indicate the 95% confidence limits for our regression.

coefficients in comparison with the width. Also, the uncertainties appear to be insignificant for the *b* and small for the *a* coefficients.

4. Comparison with previous studies

4.1. Subsurface rupture length, width and area

Several authors have proposed different empirical relationships connecting fault dimensions, derived either from surface ruptures or aftershock areas, with earthquake magnitudes (Ms or Mw) for Greece and the surrounding regions. On the other hand, Wells and Coppersmith (1994) compiled a large dataset consisting of 244 earthquakes from around the world, along with reliable estimates of their source dimensions and moment magnitudes. They developed a series of empirical relationships for fault length, width, area, maximum and average displacement for the whole of their dataset but also separately for each faulting-type group (normal, thrust, strike-slip). As stated earlier, their results indicated that there is no significant difference between the relationships derived for

individual faulting-types and those derived for the whole dataset, thus we use in our comparison only the latter ones. Table 4 gives a list of the published empirical relationships that we refer to in this paper.

The significance of the differences between the relationships we derived and those suggested by other authors was tested using a statistical F-test. The null hypothesis employed by this test is that the variances of the two distributions are equal, therefore it is expected that they should have originated from the same model. The ratio F of the variances is then calculated along with the probability that indicates how significantly this value diverges from the null hypothesis. Based on this probability we can either accept or reject the null hypothesis that the two distributions are similar. We chose not to perform an additional t-test that is used to check two distributions for significantly different mean values because such a test would depend on the a regression coefficients that exhibit a much larger error when compared to the b coefficients (by a factor 6.7–9, see Table 3).

Table 4
Summary of log (L, W, A)–M empirical relationships refered to in this study

Relationship	Region	Validity	Reference
SbRL			
log $L=-2.55+0.61$Ms	Greece	5.8–7.5	Kiratzi et al. (1985)
log $L=-1.85+0.51$Mw	Greece	5.5–7.5	Papazachos and Papazachou (1997)*
log $L=-2.44+0.59$Mw	Global	4.8–8.1	Wells and Coppersmith (1994)
log $L=-0.79+0.35$Ms	Greece	5.5–7.1	Drakatos and Latousakis (2001)
SbRW			
log $W=-0.13+0.19$Mw	Greece	5.5–7.5	Papazachos and Papazachou (1997)*
log $W=-1.01+0.32$Mw	Global	4.8–8.1	Wells and Coppersmith (1994)
SRL			
log $l=-3.22+0.69$Mw	Global	5.2–8.1	Wells and Coppersmith (1994)
log $l=-4.09+0.82$Ms	Middle–East	5.5–7.9	Ambraseys and Jackson (1998)
log $l=-3.93+0.78$Ms	Aegean area	5.6–7.2	Pavlides and Caputo (2004)
RA			
log $A=-2.73+0.81$Ms	Greece	5.8–7.3	Kiratzi et al. (1985)
log $A=-3.49+0.91$Mw	Global	4.8–7.9	Wells and Coppersmith (1994)

l represents rupture length determined using estimates from surface ruptures. The asterisk indicates studies where both types of data have been used (aftershock extent and surface ruptures). Header notation follows that of Table 3.

Table 5
Results of the application of an F-test to the relationships derived in this study and those suggested by other authors (see also Table 4)

Reference	F	Null hypothesis	Significance
SbRL			
Kiratzi et al. (1985)	3.03	rejected	>99%
Wells and Coppersmith (1994)	1.57	rejected	>80%
Papazachos and Papazachou (1997)	1.17	not rejected	>70%
Drakatos and Latousakis (2001)	1.00	not rejected	>82%
SbRW			
Wells and Coppersmith (1994)	1.12	not rejected	>80%
Papazachos and Papazachou (1997)	3.20	rejected	>99%
RA			
Kiratzi et al. (1985)	1.82	rejected	>86%
Wells and Coppersmith (1994)	1.26	rejected	~53%

We performed the F-test by using the predicted values of log L; log W; log A yielded by each empirical relationship for our dataset and created pairs of distributions for comparison. In Table 5 we present the F-test results for all the relationships given in Table 4, except from the last three that involve surface rupture length and are being discussed in the next section. Figs. 5, 6 and 7 give a graphical representation of the different empirical relationships derived from regional (Kiratzi et al., 1985; Papazachos and Papazachou, 1997; Drakatos and Latousakis, 2001) or global (Wells and Coppersmith, 1994) datasets compared to the results of this study. Because of their individual characteristics, we discuss separately the results of the F-test for each of the proposed relationships. It should be noted that the data overlap between our study and the 'regional' studies mentioned previously did not exceed 25%.

- Kiratzi et al. (1985). The F-test indicates a difference with our log L–Ms relationship at a very

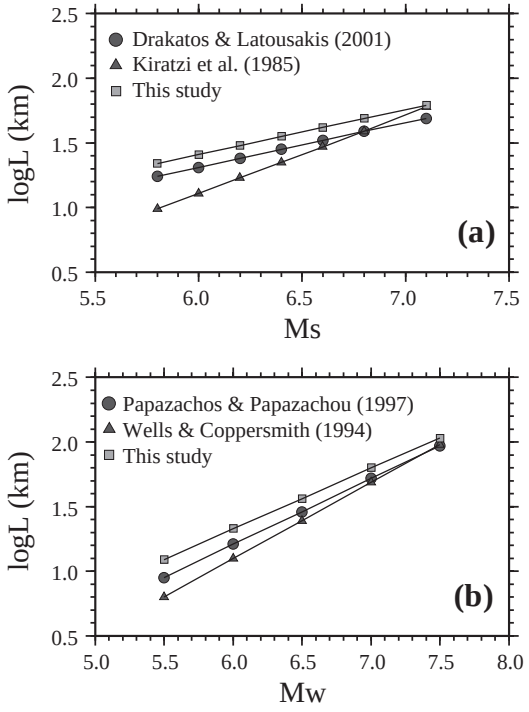

Fig. 5. (a) Comparison of log L–Ms empirical relationships, suggested by other authors, with the results of this study. Relationships are plotted inside their common validity magnitude range, (b) the same for log L–Mw relationships.

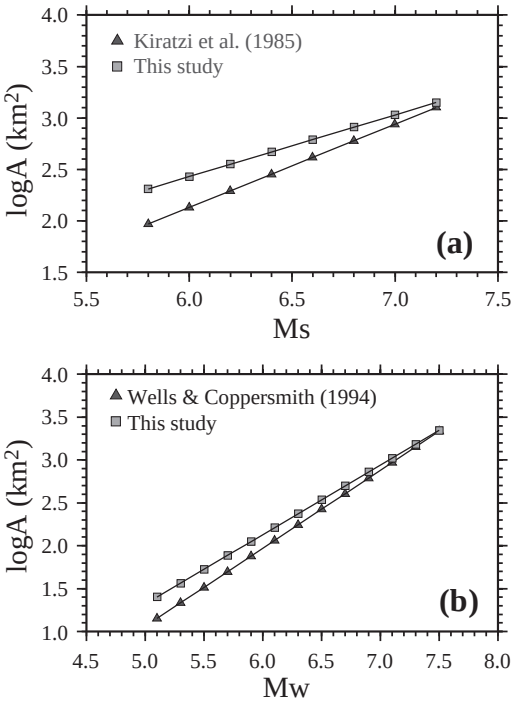

Fig. 7. Same as in Fig. 5 for (a) log A–Ms, (b) log A–Mw relationships.

significant level (>99%), therefore rejecting the null hypothesis. An inspection of the plot comparing our relationship with the one suggested by Kiratzi et al. (1985) shows large differences in the predicted values of log L for magnitudes lower than Ms ~6.5 (Fig. 5a). We also obtained a similar, but less statistically significant result (>86%) for the log A–Ms relationships, again observing larger differences in predicted rupture area values for events with magnitudes lower than 6.5 (Fig. 7a).

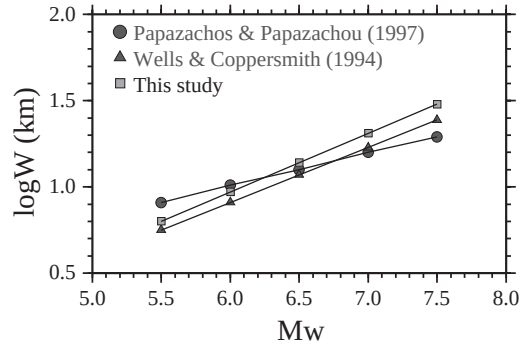

Fig. 6. Same as in Fig. 5 for log W–Mw empirical relationships.

- Drakatos and Latousakis (2001). Here the F-test shows no difference between this relationship and ours at a significance level of 82%. It should be noted that the authors used as data in their regression, 44 rupture length estimates obtained from a catalogue of aftershock sequences in Greece for the period 1971–1997, compiled by the Geodynamics Institute of the National Observatory of Athens. Their initial empirical relationship involved local magnitude (M_L), which was converted to Ms using the equation $Ms=M_L+0.5$ (Papazachos et al., 1997). It appears from Fig. 5a that our log L–Ms relationship predicts larger length values, by a factor of 1.25 (independent of magnitude since the two lines are parallel).
- Papazachos and Papazachou (1997). The results of the statistical test show for our log L–Mw relationship that the null hypothesis is not rejected, however, the significance for this is rather low (>70%). A comparison of the two lines in Fig. 5b

indicates that as in the case of Kiratzi et al. (1985), the two relationships seem to predict quite different values of length for earthquakes with Mw<6.5. On the contrary, we can reject the null hypothesis of a similarity between the fault width relationships at a high significance level (>99%).

- Wells and Coppersmith (1994). The F-test shows a difference between our log L–Mw relationship and that derived from global data, at a level of significance higher than 80%. As in the previous cases this difference seems to become larger for smaller earthquakes as shown in Fig. 5b. On the contrary, the log W–Mw relationships seem to yield practically the same values as indicated by the F-test, at a significance level greater than 80%. The log A–Mw relationships appear to show a similar trend to the rupture length with decreasing differences as magnitude increases (Fig. 7b). The F-test rejects the null hypothesis that these rupture area values come from the same distribution, at a very low significance level (~53%), however.

4.2. Surface rupture length

We did not try to make any comparison, by means of an F-test, between our relationships and those derived from surface ruptures since (1) they represent two different approaches in the determination of fault length, namely the geological and the seismological one, (2) for a range of magnitude values they yield quite different results. Instead we tried to quantify this difference by considering the variation of the ratio of the fault length derived from aftershock area extent (L) and that derived from surface ruptures (l) as a function of magnitude. This ratio can be easily deduced from the corresponding log l–Ms relationships suggested for Greece and the surrounding regions (Table 4) and the log L–Ms relationship obtained in this study (Table 3) and is

$$L/l = 2511.8 \times 10^{-0.47\mathrm{Ms}},$$
$$L/l = 1737.8 \times 10^{-0.43\mathrm{Ms}} \quad (5)$$

where the left-hand side equation gives this ratio for the Ambraseys and Jackson (1998) relationship, while the right-hand side for the one suggested by Pavlides and Caputo (2004). We also estimated in the same way this ratio using the expressions of log L and log l published by Wells and Coppersmith (1994) for global data and obtained

$$L/l = 6.0 \times 10^{-0.1\mathrm{Mw}}. \quad (6)$$

Fig. 8 shows the graphical representation of all these equations and reveals two main differences between these length ratio types. First, the 'regional' ratio values for magnitudes smaller than 6.5 appear to be several times larger than that of the 'global' one. Second, the value of 1 which implies same estimates of aftershock zone and surface rupture length, is reached at different magnitude values for the regional (Ms ~7.2 for the Ambraseys and Jackson equation, while for Pavlides and Caputo unity is not reached inside the valid magnitude range) and global ratio (Mw ~7.7–7.8).

One explanation for this result may be the larger number of earthquakes with Mw>7.2 existing in the

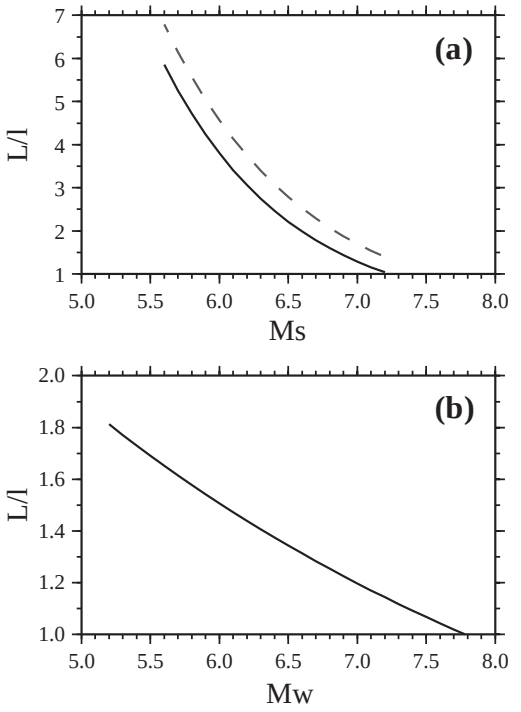

Fig. 8. (a) The 'regional' ratio of subsurface rupture length to surface rupture length. The solid curve was calculated using the Ambraseys and Jackson (1998) empirical relationship, while the dashed one using the Pavlides and Caputo (2004) equation. Both curves are plotted inside their common validity magnitude range. (b) The same for the 'global' ratio. The curve was calculated using the Wells and Coppersmith (1994) relationships.

Wells and Coppersmith dataset, that have long surface rupture lengths and therefore may create a bias towards larger values of l. In order to check this possibility, we excluded from their original dataset all events with Mw>7.2 and recalculated the regression lines for l, but also L for consistency, thus obtaining

$$\log L = -2.19 + 0.54\mathrm{Mw},$$
$$\log l = -2.95 + 0.64\mathrm{Mw} \quad (7)$$

The new equation describing the variation of the length ratio as a function of Mw is $L/l = 5.75 \times 10^{-0.1\mathrm{Mw}}$, which is almost the same with the one presented earlier. Therefore, it appears that this difference in surface and subsurface length estimates between regional and global data is not an artifact and implies that surface rupture lengths for earthquakes with Mw<6.5 in the Mediterranean Sea region are much smaller than the global average.

5. Rupture area, seismic moment and stress drop

In this section we try to establish a relationship between rupture area and seismic moment for our dataset and compare our results with those of Kiratzi et al. (1985), in an effort to infer the level of stress drop for events occurring in the Mediterranean Sea region. We decided to use in our regression the values of seismic moment reported by Harvard, for the following reasons: first, the Harvard database is the most complete of the existing worldwide moment tensor catalogues, spanning a period from 1976 until now, covering most of the occurrence period of the events under study; second, for each moment tensor solution it provides error assessment measurements that can be used to select only the well-constrained solutions.

Frohlich and Davis (1999) examined under what conditions would a moment tensor solution, reported by different agencies and institutes, be considered as well-constrained. The authors concluded that for the Harvard catalogue three such conditions should be fullfilled: (1) a quantity termed 'relative error' (E_{rel}) and defined as (Frohlich and Davis, 1999; Eq. 13 in Kagan, 2003)

$$E_{\mathrm{rel}} = \sqrt{\frac{\sum_{i,j} E_{ij}^2}{\sum_{i,j} M_{ij}^2}} \quad (8)$$

(where M_{ij} and E_{ij} are the moment tensor components and their corresponding errors) should be smaller than 0.15; (2) the measure of the strength of the non-double-couple component given by the dimensionless parameter ϵ

$$\epsilon = \frac{-\lambda_2}{\max(|\lambda_1|, |\lambda_3|)} \quad (9)$$

(where λ_1, λ_2, λ_3 are the diagonal elements of the moment tensor in the principal axis coordinate system, ordered such that $\lambda_1 \geq \lambda_2 \geq \lambda_3$) should have a value less than 0.20; (3) all six elements of the deviatoric moment tensor should be free parameters in the inversion. Obviously, conditions (1) and (3) are the most important in our case, since we are interested only in the norm (scalar seismic moment) of the moment tensor solution.

We applied these criteria to the 33 events that a corresponding moment tensor entry existed in the Harvard catalogue (events 1 and 2 occurred before 1976 and event 30 was too small to have a teleseismic solution) and found that 26 (78%) of them fulfilled these conditions. Using these values of seismic moment and the rupture area given in Table 1 we found the following relationship after the regression

$$\log A = 0.43(\pm 0.06)\log M_0 - 8.46(\pm 1.58),$$
$$r = 0.82 \quad (10)$$

which is valid for seismic moments between 5×10^{24}–5×10^{27} dyn cm (Fig. 9a).

Fig. 9b compares the above relationship with the one suggested by Kiratzi et al. (1985) for earthquakes in Greece and also includes the log A–log M_0 lines corresponding to circular faults assuming constant values of stress drop each time. It is evident that while the relationship of Kiratzi et al. (1985) predicts a constant stress drop equal to 10 bar, our relationship implies that it may actually vary as a function of seismic moment. For small to moderate earthquakes ($M_0 < 10^{26}$ dyn cm or Mw<6.6) the stress drop appears to fluctuate around the value of 10 bar, but for larger events it tends to increase to values up to 60 bar. This result seems to agree with calculated values of stress drop, e.g. 70 bar for event 35 of our dataset (Umutlu et al., 2004). However, due to the inherent uncertainties involved in the calculation of stress drop, such comparisons may be valid only for the purpose

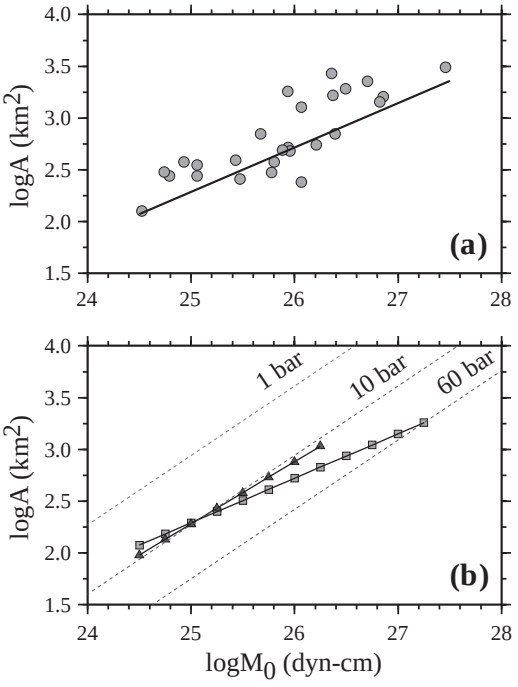

Fig. 9. (a) Diagram of the logarithm of rupture area A, shown in Table 1 versus the logarithm of seismic moment M_0 for the 26 selected events from our dataset (see text for more details). Solid line indicates the least-squares fit to the data. (b) Comparison of log A–log M_0 relationships suggested by Kiratzi et al. (1985) (black triangles) and this study (gray squares) plotted inside their individual validity magnitude range. Dashed lines represent the log A–log M_0 relationship for circular faults assuming a constant stress drop value each time.

of showing a general trend rather than predicting absolute values.

6. Concluding remarks

Based on the characteristics of our dataset, the regression results and their comparison with empirical relationships suggested by other authors we can summarize the conclusions of this study as follows:

1. Contrary to some previously published studies we did not find any evidence that the faulting type of an event may have an influence on its estimated fault dimensions. This result confirms similar findings by Wells and Coppersmith (1994) for their global dataset, or by Dowrick and Rhoades (2004) for their New Zealand regional dataset.
2. Subsurface rupture lengths versus moment/surface magnitude show the best linear correlation (0.92–0.90) followed by the rupture area (0.89–0.90). The width shows lower linear correlation values for both types of magnitudes (0.79–0.80) and one possible reason for this may be the location errors of the aftershock sequence events that may have led to an over- or underestimation of the true aftershock area width.
3. In general, the differences given by the F-test, between the relationships presented in this paper and those suggested previously, do not exhibit very high significance (>95%). This is mainly due to the fact that for magnitudes larger than approximately 6.5 all of them tend to yield similar values of source dimensions, while the differences appear in smaller magnitudes. However, we can clearly observe some degree of similarity between our log L–Ms relationship and that of Drakatos and Latousakis (2001) or difference for the corresponding log L–Mw relationship of Wells and Coppersmith (1994). This difference between regional and global relationships can be interpreted as the result of regionally variable source dimensions. Such an interpretation is supported by the observation of Papadopoulos et al. (2003) that the predicted subsurface rupture length yielded by the Wells and Coppersmith relationship (19 km) was too small compared to the observed aftershock area length (~35 km) of the 14 August 2003, Mw=6.2 Lefkada earthquake in Western Greece.
4. Regional empirical relationships for Greece and the Middle East seem to predict that the length of the aftershock area will be approximately equal to the surface rupture length of the fault for an earthquake of Ms ~7.2, while for magnitudes smaller than 6.5 the former length is several times larger than the latter. This is completely different from what is predicted by the global relationships of Wells and Coppersmith (1994), where the ratio of the two length estimates approach unity at Mw ~7.7–7.8 and for magnitudes smaller than 6.5 the aftershock area length is at maximum 1.8 times larger than the surface rupture length. This may be an overlooked sign of regional variation of fault dimensions when compared to a global average.

5. Based on the log A–log M_0 relationship we established for our dataset, it can be shown that for earthquakes smaller than Mw ~6.6 the stress drop appears to obtain a value around 10 bar in agreement with the result of Kiratzi et al. (1985). For larger events a trend of increasing stress drop is predicted, even though it is difficult to infer absolute values. From the seismic hazard point of view the conclusion of Kiratzi et al. (1985) that large earthquakes in Greece seem to cause only limited casualties and damage due to their low stress drop, remains valid. However, our results combined with knowledge of the seismotectonics of the Greek region indicate that this may be so only because events with Mw higher than 6.6 occur rarely in Greece.

Acknowledgements

This research was partly supported by the National Science Council of Taiwan in the form of a research fellowship awarded to the first author. We would like to thank Cheng-Horng Lin, Riccardo Caputo, Spyros Pavlides and Sebastian Hainzl for their careful reviews that improved this manuscript substantially. The figures of this paper were plotted using the GMT software package (Wessel and Smith, 1991).

Appendix A

This appendix gives a summary of the information available for each of the 36 aftershock sequences that were used for the derivation of the empirical relationships presented in this paper.

A.1. 1954/09/09 Algeria (no. 1 in Tables 1, 2)

The main core of information comes from Dewey (1990) who relocated the aftershocks that occurred during the first 24 h of the sequence, using teleseismic travel times and the Joint Hypocentre Determination (JHD) method. The author reported the accuracy of the relocation to be better than 3 km horizontally and also estimated the downdip depth extent of the aftershock zone to be around 7–10 km.

A.2. 1968/02/19 N. Aegean Sea (no. 2)

Drakopoulos and Economides (1972) located the largest aftershocks of the sequence using as data phases from stations in Greece and neighbouring countries, however their estimated horizontal error was of the order of 22 km. Even though this precluded the use of this event for any calculation of fault width (and fault area), it was still possible to make an estimation of the subsurface fault length by jointly considering their location results and what is known about the seismotectonics of this area. The epicentres in the south part of the aftershock zone (near the island of Skyros) were discarded, since according to Papadopoulos et al. (2002) at that area the main faulting trend is perpendicular (NW–SE) to that of the North Anatolian Fault branch (NE–SW) in which this earthquake originated. Therefore these events are either mislocated or belong to a different fault system that was triggered by the earthquake under study. Also, the epicentres to the north of the aftershock zone around the island of Lemnos appear quite scattered and were also discarded. This leaves the central part of the located aftershock zone that has a length of 95 km.

A.3. 1976/05/06 Friuli, Italy (no. 3)

Cipar (1980) used the ISC locations of the largest aftershocks recorded during the first 24 h and defined a zone with dimensions $L=30$ km, $W=18$ km. He also used synthetic seismograms and included the effect of source finiteness in order to find that the fault length for this event should be in the range of 16–24 km. Aoudia et al. (2000) relocated these largest aftershocks using the JHD method and found that the dimensions of the aftershock area are $L=25$ km, $W=15$ km with a downdip depth extent of 14 km, in reasonable agreement with the previous author.

A.4. 1978/06/20 N. Greece (no. 4)

The earthquake caused significant damage to the nearby city of Thessaloniki and therefore its aftershock sequence was closely monitored and studied. Soufleris et al. (1982) used data recorded by a

temporary local network to locate the aftershocks from 20 July until 31 August. They reported location uncertainties (both horizontally and vertically) of less than 2 km and their results defined an aftershock zone with dimensions $L=28$ km, $W=14$ km. Carver and Bollinger (1981) used their dataset to infer the space–time distribution of the aftershock sequence and concluded that the downdip depth extent should be around 12–14 km. Taking a different approach Kulhánek and Meyer (1981) analysed the spectra of teleseismic waveforms and estimated the fault length to be 32 km, close to the value yielded by the aftershock zone distribution.

A.5. 1979/04/15 Montenegro (no. 5)

Using data from a regional network, Console and Favali (1981) located the aftershocks of this event for the period 15 April until 6 May. They estimated the accuracy of their locations to be better than 5 km horizontally and 10 km vertically, while the source dimensions based on their results is $L=87$ km, $W=25$ km. Karakaisis et al. (1984) also used travel times from regional networks around Montenegro in order to locate the aftershock sequence for the period 15 April to 30 May. Their horizontal errors are of the order of 2 km and the dimensions of the resulting aftershock zone is $L=83$ km, $W=23$ km.

A.6. 1980/02/29 S. France (no. 6)

The event and its aftershock sequence was recorded by a dense local network for the period from 29 February until 9 March. Reported horizontal errors were smaller than 1 km, while the vertical ones were of the order of 3 km. Gagnepain-Beyneix et al. (1982) estimate a downdip depth extent of the aftershocks to be around 5 km.

A.7. 1980/07/09 Volos, Greece (no. 7)

Papazachos et al. (1983) used travel times of data recorded at stations in Greece and neighbouring countries in order to locate the aftershock activity for the period from 9 July until 17 August. Their reported location accuracy was 2 km horizontally and 3 km vertically.

A.8. 1980/10/10 Algeria (no. 8)

Again our main source of information is Dewey (1990) following the same method and having the same error estimates as for event 1, described above.

A.9. 1980/11/23 Irpinia, Italy (no. 9)

Many different authors have studied the aftershock sequence of this large event and different source dimension estimates were available. Scarpa and Slejko (1982) used data from a dense local network and located aftershocks for a long period of time (23 November–30 April 1981), however they do not specify any error assessment and their dimension estimates are $L=57$ km, $W=14$ km. On the other hand, Deschamps and King (1983) used data from a local network and located aftershocks for a much shorter period (30 November until 3 December). They estimate the location errors to be smaller than 2 km horizontally and about 3 km vertically, while the source dimensions based on their results are $L=50$ km, $W=14$ km. Amato and Selvaggi (1993) relocated most of the aftershocks using a 3D tomographic model (thus having a better accuracy than the authors cited previously) and the estimated dimensions of the aftershock zone are the same with the ones given by Deschamps and King (1983). Based on their results the estimated downdip extent of the aftershock area is around 14 km.

A.10. 1981/02/24 C. Greece (no. 10)

This earthquake occurred near the capital of Greece, Athens and its aftershock sequence and source properties were extensively studied. The event was almost immediately followed by a strong aftershock occurring near the epicentral area of the mainshock, but also triggered a large event in a nearby fault zone some days afterwards. This created confusion as to the real extent of the aftershock zone of the mainshock. King et al. (1985) used data from a temporary network and located aftershocks occurring from 4 March until 10 April, reporting horizontal and vertical errors of 2 and 4 km, respectively. The authors consider the whole of the aftershock zone

including the triggered event and its aftershocks, thus obtaining source dimensions of $L=60$ km, $W=20$ km. On the contrary, Papazachos et al. (1984a) used regional data from Greece and neighbouring countries and located the largest aftershocks reporting similar error estimates with King et al. (1985), however separating the aftershock zones of the mainshock and that of the triggered event. This allowed the estimation of more reasonable dimensions for an event of this magnitude with $L=32$ km, $W=15$ km. These values are also in agreement with the extent of the aftershock zone formed by the ISC located aftershocks during the first 24 h of the activity (Kim et al., 1984).

A.11. 1981/12/19 C. Aegean Sea (no. 11)

Papazachos et al. (1984b) used regional data to locate the largest aftershocks for the period between 19 December and 17 January 1982. Reported errors did not exceed 3 km horizontally and 7 km vertically.

A.12. 1982/01/18 N. Aegean Sea (no. 12)

Similar with event 11, for the period from 18 January to 21 February.

A.13. 1983/01/17 W. Greece (no. 13)

Scordilis et al. (1985) used regional data to locate the largest aftershocks reporting horizontal and vertical location errors smaller than 6 km.

A.14. 1983/08/06 N. Aegean Sea (no. 14)

Rocca et al. (1985) used regional data to locate the largest aftershocks for the period between 6 August and 23 August. Reported errors did not exceed 2.5 km both horizontally and vertically.

A.15. 1984/04/29 Perugia, Italy (no. 15)

Data from a local network were used in order to locate the whole of the aftershock sequence for the period 6–10 May. Reported errors were of the order of 0.5 km horizontally and 1 km vertically. The downdip depth extent of the aftershock zone was estimated to be 6 km.

A.16. 1985/10/27 Algeria (no. 16)

Bounif and Dorbath (1998) used data from a local network and a 3D tomographic velocity model to locate the aftershock sequence of this event for the period from 30 October until 23 November. Reported errors were smaller than 1.5 km horizontally and 3 km vertically, while the downdip depth extent was estimated to be 7 km.

A.17. 1986/09/13 S. Greece (no. 17)

Two studies are available for extracting information about the aftershock sequence of this event, namely that of Papazachos et al. (1988) and Lyon-Caen et al. (1988). The first study uses regional and local data for a small period of time (13–19 September) and locates the largest aftershocks with reported errors of 2 km both horizontally and vertically. The second study uses only local data for a period of time between 18 and 27 September locating even smaller aftershocks with an accuracy of 0.6 km horizontally and 1.2 km vertically. It is interesting to note that both studies define an aftershock zone with almost the same dimensions ($L=15$ km, $W=10$–11 km) and a downdip depth extent of 8 km.

A.18. 1988/10/16 W. Greece (no. 18)

Karakostas et al. (1993) used data from a local network in order to locate aftershocks of this moderate event during the period 25–28 October. Reported errors were smaller than 3 km horizontally and around 4 km vertically, while the downdip depth extent was estimated to be 13 km.

A.19. 1988/12/07 Armenia (no. 19)

Balassanian et al. (1995) present a map of the aftershock sequence for the period between 23 December until 4 January 1989, based on the data of a US team that monitored the aftershock activity, without mentioning however, any location error assessment. The source dimensions for that zone were estimated to be $L=46$ km, $W=12$ km. Dorbath et al. (1992) presents a detailed analysis of the aftershock sequence of this event using local data for different time periods, reporting location errors of 0.5 km

horizonatlly and 1 km vertically. More importantly, the authors relocated using the master event method the early aftershocks (7–24 December) and defined an aftershock zone with the same dimensions as Balassanian et al. (1995).

A.20. 1990/05/05 Potenza, Italy (no. 20)

Data from a local network were used in order to locate aftershocks for the period between 7 and 21 May with reported locations errors smaller than 3 km both horizontally and vertically. The downdip depth extent was estimated to be 10 km.

A.21. 1992/03/13 N. Turkey (no. 21)

Eyidogan and Akinci (1999) used data from a local network for the period between 4 and 8 April and located aftershocks with a horizontal error of less than 1 km and defined a zone with dimensions $L=40$ km, $W=13$ km. Fuenzalinda et al. (1997) also used local data and located aftershocks for a longer period of time (30 March to 22 April) without mentioning any formal location errors, but stating that the residuals of located events were smaller than 0.25 s. The dimensions of their aftershock zone were smaller than the one referred to previously ($L=30$ km, $W=8$ km).

A.22. 1992/10/12 Cairo, Egypt (no. 22)

Data recorded by a local network during the period from 13 October until 3 November were used in order to locate the aftershock sequence. Reported location errors were smaller than 2.3 km both horizontally and vertically.

A.23. 1992/11/18 W. Greece (no. 23)

Data recorded by a local network for the period between 22 November to 2 December were used to locate the aftershock sequence. Reported location errors were smaller than 3 km both horizontally and vertically.

A.24. 1993/07/14 Patra, Greece (no. 24)

This event occurred in the western part of the Corinth gulf very near the city of Patra, causing only minor damages. Karakostas et al. (1994) used local data for the period from 16 until 19 July to locate the aftershock sequence, reporting horizontal location errors smaller than 3 km and vertical location errors smaller than 2.5 km.

A.25. 1994/05/26 N. Morocco (no. 25)

Calvert et al. (1997) used regional data for a period of almost 1 year after the mainshock and located all aftershocks with a grid-search method, without mentioning any error assessment. The resulting aftershock zone had dimensions equal to $L=29$ km, $W=14.5$ km. El-Alami et al. (1998) used data recorded by a local network and located aftershocks for the period between 27 May until 10 June reporting location errors that did not exceed (horizontally and vertically) 2 km. The source dimensions stemming from their analysis are a length of $L=30$ km and a width $W=10$ km, while the downdip extent was of the order of 12 km.

A.26. 1995/05/13 Kozani, Greece (no. 26)

This event caused major damage to several towns and villages in northern Greece and therefore its aftershock sequence was closely monitored. Hatzfeld et al. (1997) analysed data from a local network for the period between 19 and 25 May and located aftershocks with a horizontal accuracy better than 1 km.

A.27. 1995/06/15 Aegio, Greece (no. 27)

The earthquake caused casualties and significant damages to the nearby town of Aegio. Tselentis et al. (1996) analysed data recorded by a local permanent network for the period from 15 June until 2 July and located aftershocks with reported horizontal/vertical location errors of the order of 3 km. The source dimensions of the aftershock zone are estimated to be $L=33$ km, $W=16$ km and downdip depth extent of 12 km. Bernard et al. (1997) also used local data for a smaller period (22–28 June) and located the aftershocks with an accuracy of 1 km both horizontally and vertically. The source dimensions of their aftershock zone are smaller ($L=27$ km, $W=11$ km) which could be attributed to the smaller location errors involved.

A.28. 1995/10/01 Dinar, Turkey (no. 28)

Oncel et al. (1998) used data recorded by a local network for the period starting 1 until 13 October and located the aftershocks for this event reporting small location errors. Pinar (1998) in his study of the source properties of this event, also presents a map of the aftershock sequence that consisted of events located using data from the regional network of the Kandilli Observatory for the period 1–4 October without specifying any location error estimates. Both studies give similar fault lengths (33–35 km) and widths (20–25 km), however we chose for our regression the estimates arising from the study of Oncel et al. (1998) as their results are likely to be more accurate.

A.29. 1995/11/22 Aqaba, Syria (no. 29)

Both Fattah et al. (1997) and Hofstetter et al. (2003) present maps of the aftershock activity using for their locations local and regional data respectively. Neither of them is specifying the location procedure, the analysis time window or any error estimate while their source dimension estimates are almost the same ($L=88$ km, $W=40$ km). On the contrary, Klinger et al. (1999) give a detailed analysis of the aftershock sequence using data from a regional network of stations in Israel, Syria and Jordan allowing a very good azimuthal coverage of the seismogenic structure. For the period between late November until December the dimensions of the aftershock zone are estimated to be $L=70$ km and $W=23$ km using events with an rms residual smaller than 0.5 s.

A.30. 1996/04/03 Irpinia, Italy (no. 30)

The phase data come from both local and regional stations in Italy for a period between 3 April until 30 June and formal location errors smaller than 1 km horizontally and around 1 km vertically (Cocco et al., 1999).

A.31. 1997/09/26 Umbria, Italy (no. 31)

The aftershock sequence of this event has been studied by several authors that have used both local and regional data and different time windows for their analysis. Amato et al. (1998) analysed local data for a period from 26 September until 31 December and reported location errors that did not exceed 1 km both horizontally and vertically. The aftershock area dimensions stemming from their results are $L=39$ km, $W=14$ km, however they acknowledge that the seismogenic fault length inferred from the seismic moment is in the range of 25–30 km. A second study by Cattaneo et al. (2000) based on local and regional travel times, gives somewhat smaller aftershock area dimensions ($L=34$ km, $W=12$ km) for the period between 26 September and 3 October with location errors smaller than 0.5 km. Finally, Deschamps et al. (2000) used local phase data in the time interval 26–30 September to locate aftershocks with a horizontal accuracy better than 0.7 km and a vertical equal to 1.5 km. The aftershock area dimensions derived from their results are smaller than the ones given previously ($L=25$ km, $W=11$ km). One reason for this difference may be a significant aftershock area expansion that may have biased the previous estimates towards larger values, thus we chose to include in our regressions the latter ones. All the studies mentioned above consistently give a downdip depth extent of 9 km for the located aftershocks.

A.32. 1998/06/27 Adana, Turkey (no. 32)

Local network data were used in order to locate the aftershock sequence for the period from 27 June until 4 July employing a minimum 1D velocity model derived for that area. Reported errors are smaller than 5 km vertically (Aktar et al., 2000).

A.33. 1999/08/17 Izmit, Turkey (no. 33)

The source properties and aftershock sequence of this disastrous event have been studied by different research groups in great detail using mostly local data. Three of the studies cited in Table 2 (Polat et al., 2002; Ozalaybay et al., 2002; Ito et al., 2002) have located the early aftershocks of this event (17–24 August) using minimum 1D or even 3D velocity models with formal errors smaller than 1 km horizontally and 2.5 km vertically. The source dimensions derived from these results were found to be very similar ($L=155$ km, $W=20$ km). On the other hand, Güllen et al. (2002) considered a much larger time period (17 August until 12 December) and

located aftershocks reporting formal errors smaller than 3 km both horizontally and vertically. The estimated dimensions of the aftershock zone are far larger than the ones mentioned above, with $L=222$ km, $W=55$ km indicating a significant expansion of the aftershock area.

A.34. 1999/09/07 Athens, Greece (no. 34)

This event occurred very near the centre of Athens and despite its moderate magnitude it caused numerous damages and casualties. Early aftershocks (7–10 September) located using local and regional stations reveal a seismogenic structure with dimensions $L=25$ km, $W=14$ km (Papadopoulos et al., 2001). Papadimitriou et al. (2002) used local data for a longer period (September to December 1999) and located aftershocks reporting formal errors smaller than 1 km both horizontally and vertically, while their source dimensions were close to those referred to above. Tselentis and Zahradnik (2000) also used local data and located aftershocks for the period 13–25 September without specifying any formal location errors. The dimensions estimates derived from their work are, however somewhat different from the ones mentioned earlier ($L=20$ km, $W=16$ km).

A.35. 1999/11/12 Düzce, Turkey (no. 35)

Data from local network stations were used to locate the aftershock sequence of this event for the period from 12 November until 31 March reporting horizontal and vertical errors smaller than 3 km.

A.36. 2001/07/26 C. Aegean Sea (no. 36)

Papadopoulos et al. (2002) present a map of the aftershock activity from 26 July until 14 August, using the routine locations determined by the Institute of Geodynamics of the National Observatory of Athens. The dimensions of this aftershock zone are quite large for an event of this magnitude ($L=40$ km, $W=23$ km) and probably are the result of aftershock area expansion and/or mislocation of the smaller events. Roumelioti et al. (2003) relocated these events using the same travel times by employing the double-difference method and lowered the formal (horizontal and vertical) location error to 1 km.The aftershock area during the first 24 h after the mainshock had thus much smaller dimensions ($L=27$ km, $W=14$ km).

References

Acharya, H.K., 1979. Regional variations in the rupture-length magnitude relationships and their dynamical significance. Bull. Seismol. Soc. Am. 69, 2063–2084.

Aktar, M., Ergin, M., Ozalaybey, S., Tapirdamaz, C., Yörük, A., Bicmen, F., 2000. A lower crustal event in the northeast Mediterranean: The 1998 Adana earthquake (Mw=6.2) and its aftershocks. Geophys. Res. Lett. 27, 2361–2364.

Amato, A., Selvaggi, G., 1993. Aftershock location and P-velocity structure in the epicentral region of the 1980 Irpinia earthquake. Ann. Geofis. XXXVI, 3–15.

Amato, et al., 1998. The 1997 Umbria-Marche, Italy, earthquake sequence: a first look at the mainshocks and aftershocks. Geophys. Res. Lett. 25, 2861–2864.

Ambraseys, N.N., Jackson, J.A., 1998. Faulting associated with historical and recent earthquakes in the Eastern Mediterranean region. Geophys. J. Int. 133, 390–406.

Aoudia, A., Saraó, A., Bukchin, B., Suhaldoc, P., 2000. The 1976 Friuli (NE Italy) thrust faulting earthquake: a reappraisal 23 years later. Geophys. Res. Lett., 577–580.

Azzara, R., Basili, A., Beranzoli, L., Chiarabba, C., Di Giovambattista, R., Selvaggi, G., 1993. The seismic sequence of Potenza (May 1990). Ann. Geofis. XXXVI, 237–243.

Baker, C., Hatzfeld, D., Lyon-Caen, H., Papadimitriou, E., Rigo, A., 1997. Earthquake mechanisms of the Adriatic Sea and Western Greece: implications for the oceanic subduction-continental collision transition. Geophys. J. Int. 131, 559–594.

Balassanian, et al., 1995. Retrospective analysis of the Spitak earthquake. Ann. Geofis. XXXVIII, 345–372.

Bayrak, Y., Öztürk, S., 2004. Spatial and temporal variations of the aftershock sequences of the 1999 Izmit and Düzce earthquakes. Earth Planets Space 56, 933–944.

Bernard, et al., 1997. The Ms=6.2 June 15, 1995 Aegion earthquake (Greece): evidence for low-angle normal faulting in the Corinth rift. J. Seismol. 1, 131–150.

Bolt, B.A., 1978. Incomplete formulations of the regression of earthquake magnitude with surface fault rupture length. Geology 6, 233–235.

Bonilla, M.G., Mark, R.K., Lienkaemper, J.J., 1984. Statistical relations among earthquake magnitude, surface rupture length and surface fault displacement. Bull. Seismol. Soc. Am. 74, 2379–2411.

Bounif, M., Dorbath, C., 1998. Three dimensional velocity structure and relocated aftershocks for the 1985 Constantine, Algeria (Ms=5.9) earthquake. Ann. Geofis. 41, 93–104.

Calvert, A., Gomez, F., Seber, D., Barazangi, B., Jabour, N., Ibenbrahim, A., Denmati, A., 1997. An integrated geophysical investigation of recent seismicity at Al-Hoceima region of north Morocco. Bull. Seismol. Soc. Am. 87, 637–651.

Carver, D., Bollinger, G., 1981. Distribution of the seismicity related to the June 20 1978 Ms=6.5, Northern Greece earth-

quake. In: Papazachos, B.C., Carydis, P.G. (Eds.), The Thessaloniki Northern Greece Earthquake of June 20 1978 and its Seismic Sequence, Technical Chamber of Greece.

Cattaneo, et al., 2000. The 1997 Umbria-Marche (Italy) earthquake sequence: analysis of the data recorded by local and temporary networks. J. Seismol. 4, 401–414.

Cipar, J., 1980. Teleseismic observations of the 1976 Friuli, Italy earthquake sequence. Bull. Seismol. Soc. Am. 70, 963–983.

Cocco, et al., 1999. The April 1996 Irpinia seismic sequence: evidence for fault interaction. J. Seismol. 3, 105–117.

Console, R., Favali, P., 1981. Study of the Montenegro earthquake sequence (March–July 1979). Bull. Seismol. Soc. Am. 71, 1233–1248.

Darragh, R.B., Bolt, B.A., 1987. A comment on the statistical regression relation between earthquake magnitude and fault rupture length. Bull. Seismol. Soc. Am. 77, 1479–1483.

Deschamps, A., King, G.C.P., 1983. The Campania-Lucania (southern Italy) earthquake of 23 November 1980. Earth Planet. Sci. Lett. 62, 296–304.

Deschamps,, et al., 2000. Spatio-temporal distribution of the seismic activity during the Umbria-Marche crisis, 1997. J. Seismol. 4, 377–386.

Dewey, J.W., 1990. The 1954 and 1980 Algerian earthquakes: implications for the characteristic displacement model of fault behaviour. Bull. Seismol. Soc. Am. 81, 446–447.

Drakatos, G., Latousakis, J., 2001. A catalog of aftershock sequences in Greece (1971–1997): their spatial and temporal characteristics. J. Seismol. 5, 137–145.

Drakopoulos, J.C., Economides, A.C., 1972. Aftershocks of the February 19, 1968 earthquake in northern Aegean Sea and related problems,. Pure Appl. Geophys. 95, 100–115.

Dorbath, L., Dorbath, C., Rivera, L., Fuenzalinda, A., Cisternas, A., Tatevossian, R., Aptekman, J., Arefiev, S., 1992. Geometry, segmentation and stress regime of the Spitak (Armenia) earthquake from the analysis of the aftershock sequence. Geophys. J. Int. 108, 309–328.

Dowrick, D.J., Rhoades, D.A., 2004. Relations between earthquake magnitude and fault rupture dimensions: how regionally variable are they? Bull. Seismol. Soc. Am. 94, 776–788.

Efron, B., Tibshirani, R.J., 1993. An Introduction to the Bootstrap. Chapman and Hall.

Ekström, G., 1994. Teleseismic analysis of the 1990 and 1991 earthquakes near Potenza. Ann. Geofis. 25, 1971–1974.

Ekström, G., Morelli, A., Boschi, E., Dziewonski, A.M., 1998. Moment tensor analysis of the central Italy earthquake sequence of September–October 1997. Geophys. Res. Lett. 25, 1971–1974.

El-Alami, S., Tadilli, B.A., Cherkaoui, T., Medina, F., Ramdami, M., Brahim, L.A., Harnafi, M., 1998. The Al-Hoceima earthquake of May 26, 1994 and its aftershocks: a seismotectonic study. Ann. Geofis. 41, 519–537.

Elenean, K.M.A., Hussein, H.M., El-Ata, A.S.A., Ibrahim, E.M., 2000. Seismological aspects of the Cairo earthquake, 12th October 1992. Ann. Geofis. 43, 485–504.

Engdahl, E.R., Van der Hilst, R.D., Buland, R.P., 1998. Global teleseismic earthquake relocation with improved travel times and procedures for depth determination. Bull. Seismol. Soc. Am. 88, 722–743.

Eyidogan, H., Akinci, M., 1999. Site attenuation and source parameters on the North Anatolian fault zone, eastern Turkey estimated from the aftershocks of March 1992 Erzincan earthquake. J. Seismol. 3, 363–373.

Fattah, A.K., Hussein, H.M., Ibrahim, E.M., El-Atta, A.S., 1997. Fault plane solutions of the 1993 and 1995 Gulf of Aqaba earthquakes and their tectonic implications. Ann. Geofis. XL, 1555–1564.

Frohlich, C., Davis, S.D., 1999. How well are well-constrained T, B and P axes in moment tensor catalogs? J. Geophys. Res. 104, 4901–4910.

Fuenzalinda, et al., 1997. Mechanism of the 1992 Erzincan earthquake and its aftershocks, tectonics of the Erzincan basin and decoupling on the North Anatolian Fault. Geophys. J. Int. 129, 1–28.

Gagnepain-Beyneix, J., Haessler, H., Modiano, T., 1982. The Pyrenean earthquake of February 29, 1980: an example of complex faulting. Tectonophysics 85, 273–290.

Giardini, D., 1993. Teleseismic observation of the November 23, 1980 Irpinia earthquake. Ann. Geofis. XXXVI (N1), 17–25.

Güllen, L., Pinar, A., Kalafat, D., Özel, N., Horasan, G., Yilmazer, M., Isikara, A.M., 2002. Surface fault breaks, aftershock distribution, and rupture process of the 17 August 1999 Izmit, Turkey, earthquake. Bull. Seismol. Soc. Am. 92, 230–245.

Haessler, et al., 1988. The Perugia (Italy) earthquake of 29 April 1984: a microearthquake survey. Bull. Seismol. Soc. Am. 78, 1948–1964.

Hanks, T.C., Kanamori, H., 1979. A moment-magnitude scale. J. Geophys. Res. 84, 2348–2350.

Hatzfeld, et al., 1996. The Galaxidi earthquake of 18 November 1992: a possible asperity within the normal fault system of the Gulf of Corinth (Greece). Bull. Seismol. Soc. Am. 86, 1987–1991.

Hatzfeld, et al., 1997. The Kozani-Grevena earthquake of 13 May 1995 revisited from a detailed seismological study. Bull. Seismol. Soc. Am. 87, 463–473.

Hofstetter, A., Thio, H.K., Shamir, G., 2003. Source mechanism of the 22/11/1995 Gulf of Aqaba earthquake and its aftershock sequence. J. Seismol. 7, 99–114.

Howell, B.F., 1981. On the saturation of the earthquake magnitudes. Bull. Seismol. Soc. Am. 71, 1401–1422.

Ito, et al., 2002. Aftershock activity of the 1999 Izmit, Turkey, earthquake, revealed from microearthquake observations. Bull. Seismol. Soc. Am. 92, 418–427.

Kagan, Y., 2003. Accuracy of modern global earthquake catalogs. Phys. Earth Planet. Inter. 135, doi:10.1016/S0031-9201(02)00214-5.

Kanamori, H., 1977. The energy release in great earthquakes. J. Geophys. Res. 82, 2981–2987.

Kanamori, H., 1983. Magnitude scale and quantification of earthquakes. Tectonophysics 93, 185–199.

Kanamori, H., Anderson, D.L., 1975. Theoretical basis for some empirical relations in Seismology. Bull. Seismol. Soc. Am. 65, 1073–1095.

Karakaisis, et al., 1984. Properties of the 1979 Monte Negro (Southwest Yugoslavia) seismic sequence. Pure Appl. Geophys. 122, 25–35.

Karakostas, B.G., Scordilis, E.M., Papaioannou, C.A., Papazachos, B.C., Mountrakis, D., 1993. Focal properties of the October 16, 1988 Killini earthquake (western Greece). 2nd Congress of the Hellinic Geophysical Union, Florina, pp. 136–145.

Karakostas, et al., 1994. The aftershock sequence and focal properties of the July 14, 1993 (Ms=5.4) Patras earthquake. Bull. Geol. Soc. Greece XXX/5, 167–174.

Kim, W.Y., Kulhanek, O., Meyer, K., 1984. Source processes of the 1981 Gulf of Corinth, earthquake sequence from body-wave analysis. Bull. Seismol. Soc. Am. 74, 459–477.

King, et al., 1985. The evolution of the Gulf of Corinth (Greece): an aftershock study of the 1981 earthquakes. Geophys. J. R. Astron. Soc. 80, 677–693.

Kiratzi, A.A., Karakaisis, G.F., Papadimitriou, E.E., Papazachos, B.C., 1985. Seismic source parameter relations for earthquakes in Greece. Pure Appl. Geophys. 123, 27–41.

Kiratzi, A.A., Wagner, G.S., Langston, C.A., 1991. Source parameters of some large earthquakes in northern Aegean determined by bodywave form inversion. Pure Appl. Geophys. 135, 515–527.

Klinger, Y., Rivera, L., Haessler, H., Maurin, J.C., 1999. Active faulting in the Gulf of the Gulf of Aqaba: new knowledge from the Mw 7.3 earthquake of 22 November 1995. Bull. Seismol. Soc. Am. 89, 1025–1036.

Kulhanek, O., Meyer, K., 1981. Spectral study of the June 20 1978, Thessaloniki earthquake. In: Papazachos, B.C, Carydis, P.G. (Eds.), The Thessaloniki Northern Greece earthquake of June 20 1978 and its seismic sequence. Technical Chamber of Greece.

Liebermann, R.C., Pomeroy, P.W., 1970. Source dimensions of small earthquakes as determined from the size of the aftershock zone. Bull. Seismol. Soc. Am. 60, 879–890.

Lyon-Caen, H., et al., 1988. The 1986 Kalamata (South Peloponnesus) earthquake: detailed study of a normal fault, evidences for East–West extension in the Hellinic arc. J. Geophys. Res. 93, 14967–15000.

Mark, R.K., 1977. Application of linear statistical models of earthquake magnitude versus fault length in estimating maximum expectable earthquakes. Geology 5, 464–466.

Meghraoui, M., Philip, H., Albarede, F., Cisternas, A., 1988. Trench investigations through the trace of the 1980 El-Asnam thrust fault: evidence for Palaeoseismicity. Bull. Seismol. Soc. Am. 78, 979–999.

Oncel, A.O., Koral, H., Alptekin, O., 1998. The Dinar earthquake (Mw=6.2) October 1, 1995 Afyon, Turkey and earthquake hazard of the Dinar-Civril fault. Pure Appl. Geophys. 152, 91–105.

Otsuka, M., 1964. Earthquake magnitude and surface fault formation. J. Phys. Earth 12, 19–24.

Ozalaybay, S., Ergin, M., Aktar, M., Tapirtamaz, C., Bicmen, F., Yörük, A., 2002. The 1999 Izmit earthquake sequence in Turkey: Seismological and Tectonic aspects. Bull. Seismol. Soc. Am. 92, 376–386.

Papadimitriou, P., Voulgaris, N., Kassaras, I., Kaviris, G., Delibasis, N., Makropoulos, K., 2002. The Mw=6.0, 7 September 1999 Athens earthquake. Nat. Hazards 27, 15–33.

Papadopoulos, G.A., Ganas, A., Pavlidis, S., 2001. Instrumental and field observations for the determination of the seismogenic structure of the 7 September 1999 Athens earthquake. Bull. Geol. Soc. Greece XXXIV, 1457–1464.

Papadopoulos, G.A., Ganas, A., Plessa, A., 2002. The Skyros earthquake (Mw=6.5) of 26 July 2001 and precursory seismicity patterns in the north Aegean Sea. Bull. Seismol. Soc. Am. 92, 1141–1145.

Papadopoulos, G.A., Karastathis, V.K., Ganas, A., Pavlides, S., Fokaefs, A., Orfanogiannaki, K., 2003. The Lefkada, Ionian Sea (Greece), shock (Mw 6.2) of 14 August 2003: evidence for the characteristic earthquake from seismicity and ground failures. Earth Planets Space 55, 713–718.

Papazachos, B.C., Papazachou, C., 1997. The Earthquakes of Greece. Ziti editions, Thessaloniki.

Papazachos, B.C., Panagiotopoulos, D.G., Tsapanos, T.M., Mountrakis, D.M., Dimopoulos, G.C., 1983. A study of the 1980 summer seismic sequence in the Magnesia region of central Greece. Geophys. J. R. Astron. Soc. 75, 155–168.

Papazachos, et al., 1984a. Properties of the February–March 1981 seismic sequence in the Alkyonides Gulf of central Greece. Ann. Geofis. 2, 537–544.

Papazachos, B.C., Kiratzi, A., Voidomatis, P., Papaioannou, C.A., 1984b. A study of the December 1981–January 1982 seismic activity in northern Aegean Sea. Pure Appl. Geophys. XXVI, 101–113.

Papazachos, B.C., Kiratzi, A., Karakostas, B., Panagiotopoulos, D., Scordilis, E., Mountrakis, G., 1988. Surface fault traces, fault plane solution and spatial distribution of the aftershocks of the September 13, 1986 earthquake of Kalamata (southern Greece). Pure Appl. Geophys. 126, 55–68.

Papazachos, B.C., Kiratzi, A., Karakostas, B., 1997. Toward a homogeneous moment-magnitude determination for earthquakes in Greece and the surrounding area. Bull. Seismol. Soc. Am. 87, 474–483.

Pavlides, S., Caputo, R., 2004. Magnitude versus faults' surface parameters: quantitative relationships from the Aegean region. Tectonophysics 380, doi:10.1016/j.tecto.2003.09.019.

Pinar, A., 1998. Source inversion of the October 1 1995, Dinar earthquake (Ms=6.1): a rupture model with implications in seismotectonics in SW Turkey. Tectonophysics 292, 255–266.

Polat, O., Eyidogan, H., Haessler, H., Cisternas, A., Philip, H., 2002. Analysis and interpretation of the aftershock sequence of the August 17, 1999, Izmit (Turkey) earthquake. J. Seismol. 6, 287–306.

Press, W., Teukolsky, S.A., Vetterling, V.T., Flannery, B.P., 1992. Numerical Recipies in C. Cambridge University Press, Cambridge.

Rocca, A., Karakaisis, G.F., Karakostas, B., Kiratzi, A., Scordilis, E.M., Papazachos, B.C., 1985. Further evidence on the strike-slip faulting of the northern Aegean trough based on properties of the August–November 1983 seismic sequence. Pure Appl. Geophys. XXVII, 101–109.

Roumelioti, Z., Kiratzi, A., Melis, N., 2003. Relocation of the 26 July 2001 Skyros island (Greece) earthquake sequence using the double-difference technique. Phys. Earth Planet. Int. 138, doi:10.1016/S0031-9201(03)00138-9.

Scarpa, R., Slejko, D., 1982. The southern Italy November 23, 1980 earthquake: some analysis of seismological data, Published report, The Italian Geodynamics Project, Publ. Num. 503, National research Council of Italy.

Scordilis, E., Karakaisis, G., Karakostas, F., Panagiotopoulos, B., Comninakis, D.G., Papazachos, P.E., 1985. Evidence from transform faulting in the Ionian Sea: the Cephalonia island earthquake sequence of 1983. Pure Appl. Geophys. 123, 388–397.

Soufleris, C., Jackson, J.A., King, G.C.P., Scholz, C.H., Spencer, C.P., 1982. The 1978 earthquake sequence near Thessaloniki (northern Greece). Geophys. J. R. Astron. Soc. 68, 429–458.

Taymaz, T., Jackson, J., McKenzie, D., 1991. Active tectonics of the north and central Aegean Sea. Geophys. J. Int. 106, 433–490.

Tocher, D., 1954. Earthquake energy and ground breakage. Bull. Seismol. Soc. Am. 48, 147–153.

Tselentis, G.A., Zahradnik, J., 2000. The Athens earthquake of September 1999. Bull. Seismol. Soc. Am. 90, 1143–1160.

Tselentis, G.A., Melis, N.S., Sokos, E., Papatsimpa, K., 1996. The Egion June 15 (6.2 ML) earthquake, Western Greece. Pure Appl. Geophys. 147, 83–98.

Umutlu, N., Koketsu, K., Milkereit, C., 2004. The rupture process during the 1999 Düzce, Turkey, earthquake from joint inversion of teleseismic and strong-motion data. Tectonophysics 391, doi:10.1016/j.tecto.2004.07.019.

Vakov, A.V., 1996. Relationships between earthquake magnitude, source geometry and slip, mechanism. Tectonophysics 261, 97–113.

Wells, D.L., Coppersmith, K.J., 1994. New empirical relationships among magnitude, rupture length, rupture width, rupture area, surface displacement. Bull. Seismol. Soc. Am. 84, 974–1002.

Wessel, P., Smith, W., 1991. Free software helps maps and display data. EOS Trans.-Am. Geophys. Union 72, 441.